PROCEEDINGS OF ECOS 2023 - THE 36TH INTERNATIONAL CONFERENCE ON
EFFICIENCY, COST, OPTIMIZATION, SIMULATION AND ENVIRONMENTAL IMPACT OF ENERGY SYSTEMS
25-30 JUNE, 2023, LAS PALMAS DE GRAN CANARIA, SPAIN

Improving the carbon efficiency of two-stage DME synthesis based on wheat-straw gasification

René Kofler [a] *, Lasse Røngaard Clausen [a]

*[a] Section of Thermal Energy, DTU Construct, Technical University of Denmark, Kgs. Lyngby, 2800, Denmark. * renekof@dtu.dk*

Abstract:

For a future fossil-free energy system, solutions for hard-to-abate sectors like maritime transport need to be found. Dimethyl ether (DME) produced from sustainable biomass, like wheat straw, is a promising fuel for substituting fossil Diesel fuels in marine engines. In this work, biorefineries based on wheat straw gasification were designed and analysed. The biorefineries produced DME via two-stage synthesis, where syngas was first synthesized to methanol, before methanol was dehydrated to DME in a second step. In addition, bio-ash was produced, which acts as a soil amendment and carbon sink, when returned to the fields. The biorefineries included alkaline electrolysers for producing hydrogen to increase the carbon and energy efficiency of the plants. In this work, the addition of hydrogen at different process locations was investigated: 1) at high temperatures, enabling the conversion of CO_2 to CO via the reverse water gas shift reaction or 2) at low temperatures. In addition, the amount of hydrogen added through the electrolysers and the amount of gas (containing mainly H_2, CO and CO_2) purged after the methanol reactor were varied. By increasing the amount of hydrogen in the system, carbon efficiencies >98 % were achieved, independent of the location of the hydrogen addition and purge ratios used. Reducing the purge ratio enabled to produce more DME at the same amount of hydrogen added, leading to higher energy efficiencies. Hydrogen addition at low temperature achieved higher energy efficiencies compared to hydrogen addition at high temperatures, because it enabled the operation of the electrolysers at high pressures of 30 bar and reducing the electricity consumption in the compressors. In general, any measures of increasing the energy and carbon efficiency led to an increase in the size of the methanol reactor, leading to a trade-off between investment and operational costs.

Keywords:

Biofuel, Biomass gasification, Dimethyl ether (DME), Hydrogen quench, Power-to-liquid, Wheat straw

1. Introduction

A transition from the fossil fuel based energy system we live in today to an energy system based on renewable energy sources is necessary for reducing climate change. In many sectors this can be achieved by implementing electricity production from renewables, like wind and solar, and electrifying processes. However, there are hard-to-abate sectors like the maritime transport and the aviation sector, where electrification is not possible. Lund et al. [1] show that sustainable use of biomass for producing fuels for these sectors is important for achieving the decarbonization goals. For Denmark, wheat straw has been identified as an important feedstock for a sustainable production of fuels for the maritime transport sector via gasification and similar processes [1], [2].

The use of wheat straw in gasification is challenging due to a high ash content and its low melting temperature. The low-temperature circulating fluidized bed (LT-CFB) gasifier is designed for enabling the efficient conversion of difficult residual biomasses, like straw and manure [3]. In addition to the efficient conversion, the LT-CFB gasifier enables also the production of bio-ash or bio-char, which acts as a carbon sink and improves soil properties, when returned to the fields [4]. The produced gas from the LT-CFB gasifier contains a high tar content, making it unsuitable for downstream fuel synthesis without further treatment.

In our previous works, fuel production plants based on the LT-CFB gasifier were designed and analysed based on their carbon efficiency [5] and exergy efficiency [6]. The carbon efficiency describes, how much of the carbon in the feedstock (i.e. wheat straw) is ending up in the produced fuels and bio-ash. This value is an important measure, because plants with a high carbon efficiency enable to replace a larger part of the fossil-based fuels with the same amount of limited biomass resources. In the studies, the tars are catalytically deoxygenated and then condensed, yielding a high-quality bio-oil. The remaining tar-free gas is used to produce electricity, synthetic natural gas (SNG) or dimethyl ether (DME). In the SNG and the DME production

https://doi.org/10.52202/069564-0102

plant, electrolytic hydrogen is produced and used for increasing the amount of produced fuel. The results show that the SNG production plant reaches the highest carbon and exergy efficiencies, followed by the DME and the electricity production plant. The results show that the DME production plant suffers from an inefficient conversion of tar-free gas to DME, due to the hydrocarbons remaining in the gas after the bio-oil condensation.

The DME production plant was further investigated, because of the promising properties of DME as a substitute for fossil fuels in marine diesel engines [7]. In [8], we showed that the carbon efficiency of a DME production plant based on the LT-CFB gasifier can be increased significantly by changing the plant layout. The carbon efficiency can be improved by using a partial oxidation step after or instead of the tar deoxygenation and condensation. This enables the reforming and cracking of the hydrocarbons (and tars, in the cases without bio-oil condensation) and making the carbon available for DME synthesis. The use of two-stage DME synthesis instead of one-stage synthesis further increases the carbon efficiency. In the two-stage synthesis, methanol is first synthesized from the tar-free gas. The methanol is then dehydrated to DME and water in a second reactor. In the one-stage synthesis, both reactions are taking place in the same reactor, leading to the production of CO_2 as a by-product, reducing the carbon efficiency of the plants. Lastly, a hydrogen quench, where hydrogen is added at high temperatures directly after the partial oxidation step, can further increase the carbon efficiency. The analysis of 14 different plants showed that in most of the cases, an increase of the carbon efficiency also leads to an increase in energy efficiency. Higher efficiencies also mean that more hydrogen and hence more electricity is needed in the plants. While the study showed how the carbon efficiency can be increased by changing the plant layout, the influence of different design parameters was not investigated, due to the complexity of the study, caused by the number of plants included.

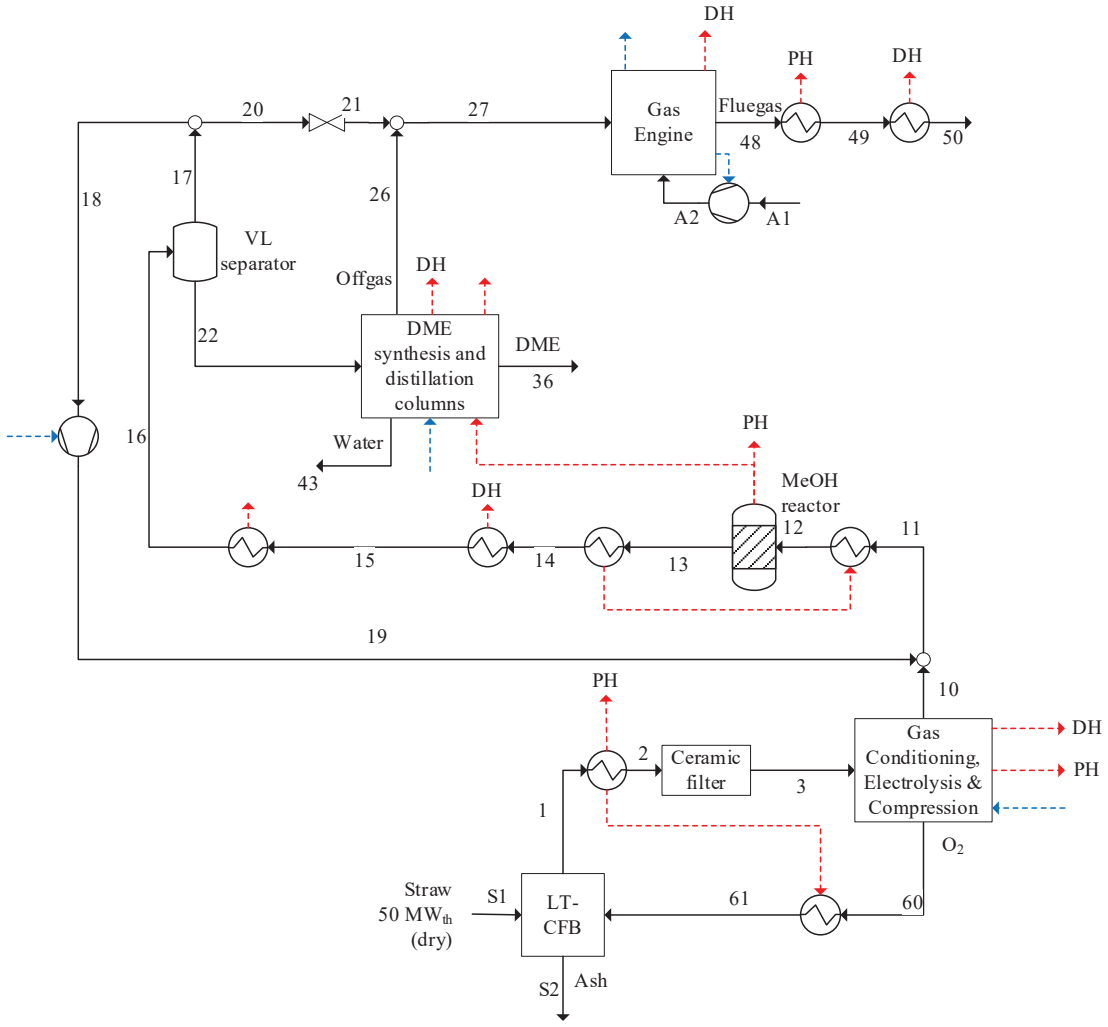

Figure 1. General flowsheet of the investigated plants. Note: The difference between the investigated plants lays in the block "Gas Conditioning, Electrolysis & Compression" as shown in Figure 3

https://doi.org/10.52202/069564-0102

In this work, two of the most promising plants were used for investigating the influence of two important design parameters, the amount of hydrogen addition and the purge ratio in the methanol synthesis loop, on the carbon efficiency and the energy efficiency. In addition, the influence of these parameters on the size of the methanol reactor, a key component in the synthesis part, was evaluated by analysing the change in mole flow rate to the reactor. The two investigated plants as well as the design parameter variation are explained in detail in the following section.

2. Methods

2.1. System layout

In this work, two different plant layouts for the production of DME and bio-ashes from wheat straw were investigated. Figure 1 shows the general plant design of the two different plant layouts. Wheat straw (stream S1) was gasified in the LT-CFB gasifier, using oxygen (61) from an alkaline electrolyser, producing a tar-laden gas (1) and bio-ash (S2). The tar-laden gas was then cooled from 660 °C to 500 °C before any remaining particles were removed in a ceramic filter. After that, the gas (3) entered a block, where the tars and hydrocarbons in the gas were cracked and reformed, before adding electrolytic hydrogen and compressing the gas to the required synthesis pressure. The pressurized gas (10) was then mixed with the recycling stream (19) and preheated before entering the methanol reactor (12).

The mixture of methanol, water and other light fractions out of the methanol reactor was then cooled down (streams 13-16) before entering a vapor-liquid (VL) separator. The vapor exiting the top (17) was split, with the major part (18) being recycled to the methanol reactor and a smaller purge stream (20) being sent to a gas engine in order to avoid the accumulation of inerts in the system. Liquid at the bottom (22) was sent to the block for DME synthesis and distillation columns. The detailed layout of the block is shown in Figure 2. The DME synthesis block yielded a DME stream (36) with a purity of 99.99 %, an offgas from the topping column (26), which is sent to the gas engine and a water stream (43) from the methanol column. The purge gas (21) and the offgas (26) were burned in a turbo charged gas engine, producing electricity and district heating, using air (A1) as oxidant. The exhaust gas (48) from the gas engine was cooled, providing district heating and process heat.

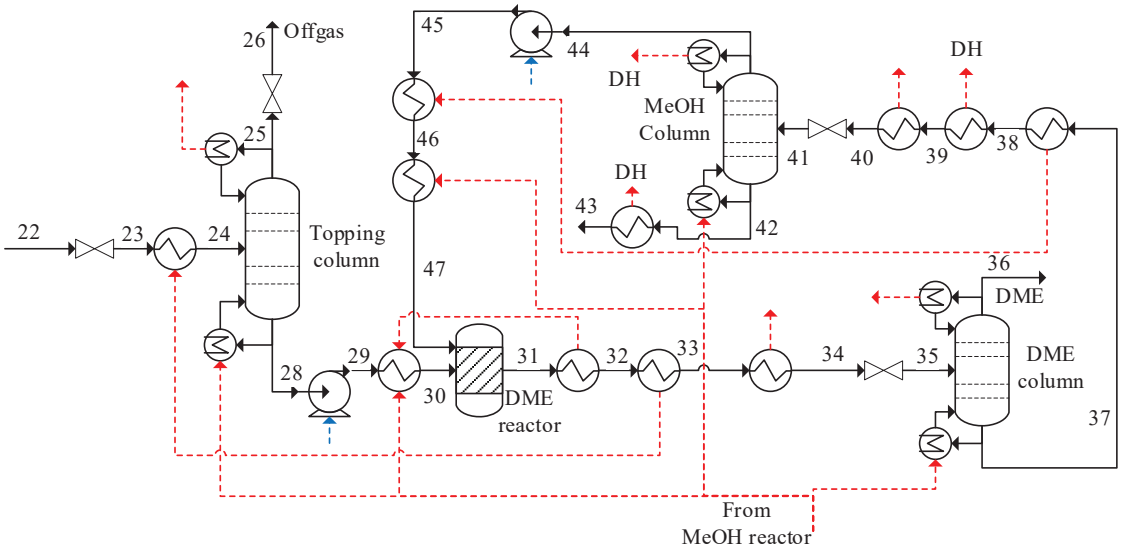

Figure 2. Detailed flowsheet of the DME synthesis and distillation columns section.

Figure 3 depicts the two different layouts for the gas conditioning block. In both cases, the tar-laden gas (stream 3) was first preheated to $T_{\mathrm{POX,preheat}} = 600\ °C$ before entering the partial oxidation (POX) reactor. Pure oxygen (52-57) from the electrolyser was used for the POX. The oxygen was also preheated to $T_{\mathrm{POX,preheat}} = 600\ °C$ and mass flow rate was controlled to reach an outlet temperature of $T_{\mathrm{POX}} = 1200\ °C$.

The differences between the two investigated layouts lay in the location of hydrogen addition. In the first layout (without hydrogen quench), hydrogen was produced in an alkaline electrolyser and added at low temperatures (51). This enabled to operate the electrolyser at a pressure of 30 bar and mixing the hydrogen with the tar-free gas after cooling and compressing the gas in a 4-stage compression with intercooling. The gas and hydrogen mixture (9) was then compressed to a pressure of 85.1 bar in the final compression stage. The high-pressure electrolysis also enabled the expansion of preheated oxygen (53) using turbines, recovering some electricity.

https://doi.org/10.52202/069564-0102

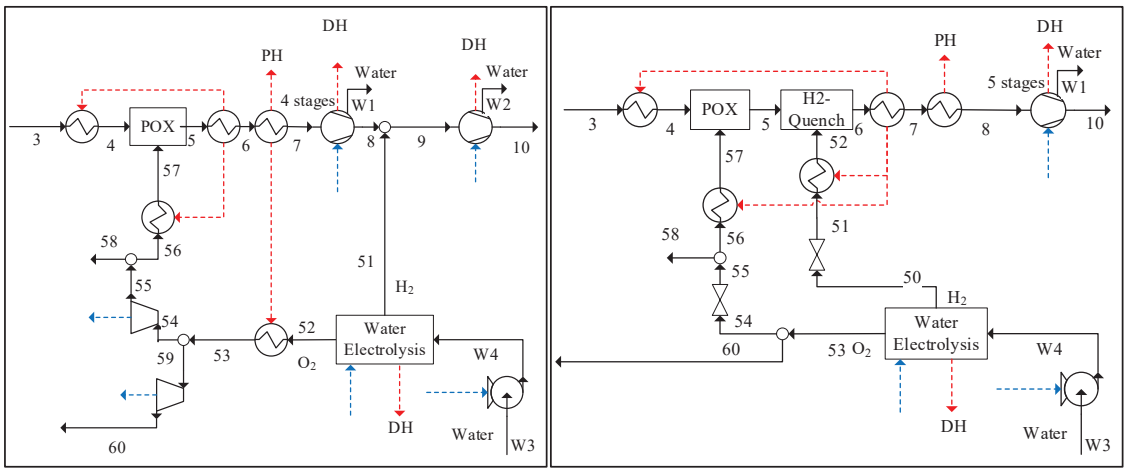

Figure 3. Flowsheet of the gas conditioning block of the two different plant layouts. Left: Plant without hydrogen quench (hydrogen addition at low temperature). Right: Plant with hydrogen quench (hydrogen addition at high temperature directly after POX).

In the second layout (with hydrogen quench), hydrogen was preheated to 600 °C and injected directly after the POX in a hydrogen quench reactor (stream 52). At temperatures above 900 °C, the reverse water gas shift (rWGS) reaction is promoted [9], leading to the conversion of CO_2 to CO, as shown in eq. (1). This process is referred to as hydrogen quench. Due to the addition of hydrogen after the POX at low pressures, the alkaline electrolysis was operated at low pressures as well.

$$CO_2 + H_2 \leftrightarrow \mathrm{CO} + \mathrm{H_2O} \qquad 41\ \mathrm{kJ/mol} \qquad (1)$$

2.2. Modelling and assumptions

The plants were modelled and simulated using the software Aspen Plus V11 [10]. The components were modelled in a zero-dimensional approach [11]. The property method RK-SOAVE (Redlich-Kwong-Soave) [12] was used for the LT-CFB gasifier, gas conditioning and gas engine, including the heat exchangers used before and after these components. SR-POLAR (Schwartzentruber and Renon) [13] was used for the remaining components. Vapor-liquid equilibrium (VLE) was assumed for all streams, except of those, where DME, methanol and water were present. In those streams vapor-liquid-liquid equilibrium (VLLE) was calculated. The solid streams and more complex liquids, namely straw, char, bio-ash, and tars were handled as so-called non-conventional streams. Non-conventional streams are only characterized by a constant heat capacity and a higher heating value (HHV) and are not considered in the chemical equilibrium. The HHV for the non-conventional compounds was estimated using eq. (2) [14], as implemented in Aspen Plus.

$$\mathrm{HHV} = [146.58\,\mathrm{C} + 568.78\,\mathrm{H} + 29.4\,\mathrm{S} - 6.58\,\mathrm{A} - 51.53(\mathrm{O} + \mathrm{N})] \cdot 10^2 \ \left[\frac{\mathrm{Btu}}{lb} = 2.326\frac{\mathrm{kJ}}{\mathrm{kg}}\right] \qquad (2)$$

In eq. (2), C, H, S, O, N and A denote the carbon, hydrogen, sulphur, oxygen, nitrogen and ash content in wt.-%, respectively.

For the plants, a wheat straw input of 50 MW_{th} based on the lower heating value (LHV) was used. That corresponded to a mass flow rate of $\dot{m}_{straw} = 3.41\ kg/s$ with the composition shown in Table 1. The LT-CFB gasifier was modelled for operating temperature of 660 °C and 700 °C in the pyrolysis and char reactor, respectively. The pyrolysis model was based on experimental data [15], while chemical equilibrium was assumed for the char reactor. The resulting gas composition was validated against the experimental results. A detailed description of modelling of the pyrolysis reactor can be found in the supplementary material of our previous work [5].

Table 1. Proximate and ultimate analysis of wheat straw pellets used as feedstock for experiments which the model was calibrated to [15].

Proximate Analysis (wt.%, as received)		**Ultimate analysis (wt.%, dry and ash free)**	
Moisture	8.5 %	N	0.8 %
Volatiles	46.2 %	C	46.2 %
Ash	6.6%	H	6.6 %
Fixed carbon	17.9 %	O	46.4 %

https://doi.org/10.52202/069564-0102

Oxygen for the LT-CFB gasifier, coming from the electrolyser was preheated to 560 °C. For heat exchangers used for preheating and cooling streams, as well as provision of process heat and district heating, $\Delta T_{Gas/Water} = 10\ K$ and $\Delta T_{Gas/Gas} = 30\ K$ were used if no other information are given. Process heat was defined as provision of saturated steam at 200 °C. For district heating, water was heated from 40 °C to 75 °C.

The electrolysers were operated at 30 bar and 1.63 bar, for the system with hydrogen addition at low and high temperatures, respectively. The pressure was set by pumping water to the respective pressure. For pumps, compressors and turbines, isentropic efficiencies of $\eta_{is} = 0.8$ and mechanical efficiencies of $\eta_{mech} = 0.94$ were used. For the electrolysers, an LHV-efficiency of 70 % was used. The electrolysers were operated at 90 °C, enabling the provision of district heating, by cooling the electrolysis stacks.

For the POX, all streams entering the POX were preheated to 600 °C. The outlet temperature was set to 1200 °C by varying the oxygen supply to the POX. The hydrogen for the hydrogen quench was preheated to $T_{\mathrm{H_2,preheat}} = 600\ °\mathrm{C}$. The outlet temperature from the hydrogen quench depended on the amount of hydrogen added. However, in all investigated cases the outlet temperature was higher than 880 °C, and hence high enough for achieving the spontaneous, non-catalytic rWGS reaction [9]. The resulting tar-free gas was then cooled and compressed to 85.1 bar in a 5-stage compression with intercooling.

A boiling-water reactor was used for the methanol synthesis. The outlet temperature was set to $T_{\mathrm{MeOH\ reactor}} = 240\ °C$. Chemical equilibrium with temperature approach was assumed for the occurring reactions shown in eq. (3) and (4).

$$4\ \mathrm{H_2} + 2\ CO \leftrightarrow 2\ CH_3OH \qquad \text{-182 kJ/mol} \qquad \Delta T_{approach} = 15\ K \qquad (3)$$

$$\mathrm{CO} + \mathrm{H_2}O \leftrightarrow CO_2 + H_2 \qquad \text{-41 kJ/mol} \qquad \Delta T_{approach} = 15\ K \qquad (4)$$

The gas stream flowing to the methanol reactor was preheated to $T_{\mathrm{preheat}} = 210\ °\mathrm{C}$. After the reactor, the stream was cooled in several heat exchangers to 25 °C before entering the vapor-liquid separator. The vapor part was then split. The biggest part was recycled to the methanol reactor, while a smaller purge stream was sent to the gas engine to avoid the accumulation of inerts in the synthesis loop. The remaining CO_2 in the liquid stream from the VL-separator was removed in a topping column after throttling, before the methanol/water mixture was pumped to a pressure of 46.1 bar and preheated to 210 °C for the DME reactor. An adiabatic reactor was used for the DME synthesis. For the methanol dehydration (eq. (5)), chemical equilibrium with temperature approach was assumed. The produced DME was purified in the DME column after cooling and throttling the stream. The bottom stream was sent to the methanol column, where methanol was separated and returned to the DME reactor while the water was disposed.

$$2\ CH_3OH \leftrightarrow CH_3OCH_3 + H_2O \qquad \text{-23 kJ/mol} \qquad \Delta T_{approach} = 100\ K \qquad (5)$$

The gas engine was turbo charged to 2 bar. The air mass flow rate to the engine was set to achieve an excess air ratio of $\lambda = 2$, assuming complete combustion. The gas engine was cooled using district heating water. The exhaust gas at 400 °C was cooled to 80 °C providing both process heat and district heating.

A more detailed description of the modelling approach for the different components and the assumptions used can be found in our previous work [8]. The plant layouts investigated in this work correspond to the plants LP_POX-2st and LP_POX-H2_QNCH-2st from [8] for the system with hydrogen addition at low and high temperatures, respectively.

2.3. Parameter variations

In this work, the influence of two key parameters in the plants were investigated: a) the amount of hydrogen added to the system; b) the amount of gas being purged from the methanol synthesis loop.

The amount of hydrogen in the system was varied by increasing the water mass flow rate of stream W3 going to the electrolyser (see Figure 3). The water mass flow rate was gradually increased from the values used in [8] (1.68 kg/s for hydrogen addition at low temperatures and 2.08 kg/s for hydrogen addition at high temperatures) to 5 kg/s. This corresponds to a variation of the hydrogen flow rate of 0.19 – 0.56 kg/s and 0.23 – 0.56 kg/s for the plant with hydrogen addition at low and high temperatures, respectively. The amount of water added to the electrolysers in [8] was determined in order to achieve an H2/CO ratio of two at the inlet of the methanol reactor (stream 12 in Figure 1).

The amount of purged gas after the vapour-liquid separator in the methanol synthesis loop was varied by varying the purge ratio between 5 %, as used in [8], and 1 %, in steps of 1 %. The purge ratio PR is defined according to eq. (6), where the stream numbers in the subscripts reference to the stream numbers shown in Figure 1.

$$\mathrm{PR} = \frac{\dot{m}_{20}}{\dot{m}_{17}} \tag{6}$$

Both variations were conducted simultaneously, meaning that for each value of purge ratio, the amount of hydrogen in the system was varied. The performance of the two plants at different hydrogen mass flows and purge ratios was evaluated by using the energy efficiency η_{main} and the carbon efficiency γ_{tot}, as defined in eq. (7) and eq. (8), respectively.

$$\eta_{\mathrm{main}} = \frac{\dot{m}_{DME} \cdot LHV_{DME}}{\dot{m}_{Straw} \cdot LHV_{Straw} + |\dot{W}_{net}|} \tag{7}$$

$$\gamma_{\mathrm{tot}} = \frac{\dot{m}_{C,DME} + \dot{m}_{C,Bio-ash}}{\dot{m}_{C,Straw}} \tag{8}$$

In addition to the efficiencies, the influence of the variations on the investment cost and the operational cost was estimated. For the investment cost, the biggest variation within each plant was expected to be experienced in a change in methanol reactor size. The size of the reactor was assumed to be proportional to the inlet volume flow rate of the reactor. Since the inlet temperature and pressure were equal for all investigated plants, the volume flow rate was proportional to the inlet mole flow rate to the reactor. In order to estimate the change in reactor size for the different simulations, the relative increase $\varepsilon_{\mathrm{Reactor}}$ was calculated according to eq. (9), where $\dot{n}_{12}$ denotes the inlet mole flow rate to the methanol reactor for the investigated plant and $\dot{n}_{12,\mathrm{ref}}$ denotes the inlet mole flow rate to the methanol reactor for the reference plant. The plant with hydrogen addition at high temperatures (with quench) from [8], corresponding to the plant with hydrogen quench and a purge ratio of 5 % was used as reference case.

$$\varepsilon_{\mathrm{Reactor}} = \frac{\dot{n}_{12} - \dot{n}_{12,\mathrm{ref}}}{\dot{n}_{12,\mathrm{ref}}} \tag{9}$$

For the operational cost, the variation in the net electricity consumption was used as a measure, because the biomass used was kept constant for the investigated plants. The variation was estimated by looking at the increase in net electricity consumption $\varepsilon_{\mathrm{EL}}$, as calculated in eq. (10). $\dot{W}_{\mathrm{net}}$ denotes the net electricity consumption of the investigated plant and $\dot{W}_{\mathrm{net,ref}}$ denotes the net electricity consumption of the reference plant.

$$\varepsilon_{EL} = \frac{\dot{W}_{\mathrm{net}} - \dot{W}_{\mathrm{net,ref}}}{\dot{W}_{\mathrm{net,ref}}} \tag{10}$$

3. Results

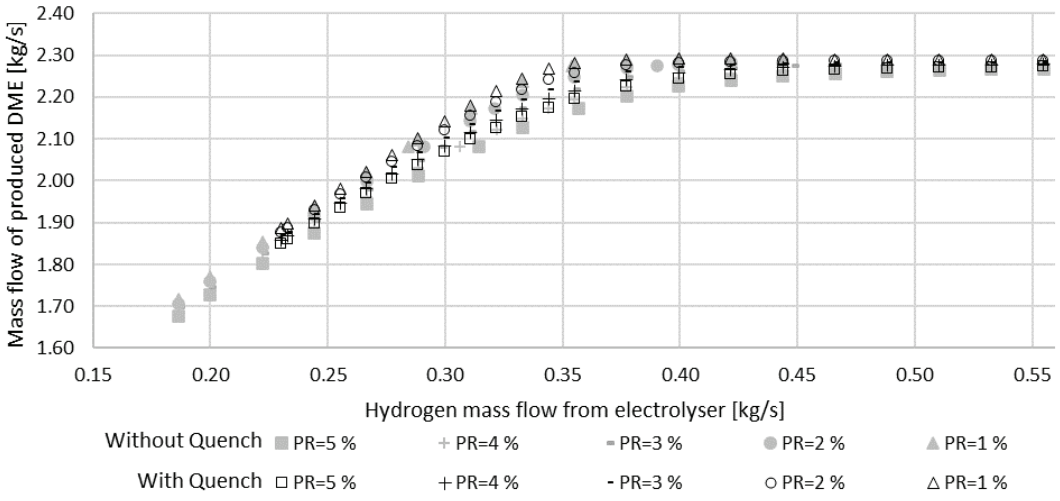

Figure 4. Mass flow rate for produced DME over hydrogen mass flow rate added by the electrolyser for the two different plants at different purge ratios (PR). Note: the grey, filled symbols denote the plant with hydrogen addition at low temperature (without quench), while the black, empty symbols denote the addition at high temperature (with quench).

https://doi.org/10.52202/069564-0102

In this section, the results of the conducted parameter variations are shown. Figure 4 shows the mass flow rate of produced DME for different hydrogen mass flows from the electrolyser. The grey, filled symbols show the results for the plant with hydrogen addition at low temperatures (without quench) and the black, empty symbols show the results for hydrogen addition at high temperatures (with quench). The different symbols denote the different purge rates (PR) used in the methanol synthesis loop.

The amount of produced DME increased with increasing hydrogen addition. The trend of the increase was similar for all the investigated plants and purge ratios with a strong increase in DME production up to a hydrogen addition of around 0.35 kg/s to 0.4 kg/s before flattening towards a maximum achievable DME flow rate. The results show that a decrease in the purge ratio increases the amount of DME produced at constant hydrogen flow rate added as well as the maximum achievable DME mass flow. It can also be seen that in the plants with hydrogen addition at high temperatures (with quench), more DME was produced when adding the same amount of hydrogen, compared to the plants without quench. The difference was more distinct with higher purge ratios, while the difference was almost negligible for a purge ratio of 1 %.

As it can be seen in eq. (8), an increase in DME production led to an increase in carbon efficiency, since the other two carbon flows in the system were kept constant for all plants, i.e. the carbon flows in wheat straw and bio-ash. Hence, an increase in hydrogen addition through the electrolyser led to an increase in carbon efficiency, and a reduction in purge rate led to a higher carbon efficiency at constant hydrogen addition.

Figure 5 shows the energy efficiency of the plants over the carbon efficiency. Based on the results from Figure 4, we know that moving from left to right, i.e. from lower to higher carbon efficiencies, was equivalent to adding more hydrogen to the system. In Figure 5, it can be seen that by reducing the purge rate, higher energy efficiencies were reached for achieving the same carbon efficiency. This was connected to requiring less hydrogen in the system for yielding the same DME production, leading to a reduction in electricity used for the electrolysers and hence a lower net electricity consumption (see also Figure 6). Additionally, the diagonal lines visible in Figure 5 show that reducing PR at constant hydrogen addition led to an increase in both energy and carbon efficiency. That shows that using low purge ratios is very beneficial for improving the performance of the plants.

With increasing carbon efficiencies, the energy efficiency slowly increased until reaching a maximum at different locations for different plants and purge ratios and started decreasing slowly until it reaches a rapid fall at high carbon efficiencies. For a purge ratio of 1 %, the energy efficiency was almost constant for both plants up to a carbon efficiency close to 98 % before rapidly falling at higher carbon efficiencies. This introduced the possibility to yield almost all of the carbon in the straw to end up in DME and bio-ash. For higher purge ratios, the decrease in energy efficiency started earlier. The strongest decrease was seen for a purge ratio of 5 %, where a significant reduction was already seen around a carbon efficiency of 90 %.

At very high carbon efficiencies, a rapid decrease in energy efficiency with little to no increase in carbon efficiency can be observed. This area corresponded to the part of Figure 4, where no additional DME was produced by adding more hydrogen to the system. With purge ratios of 4 % and 5 %, the rapid decrease in energy efficiency occurred earlier, and it was not possible to achieve carbon efficiency of 99 %, no matter how much hydrogen was added to the system.

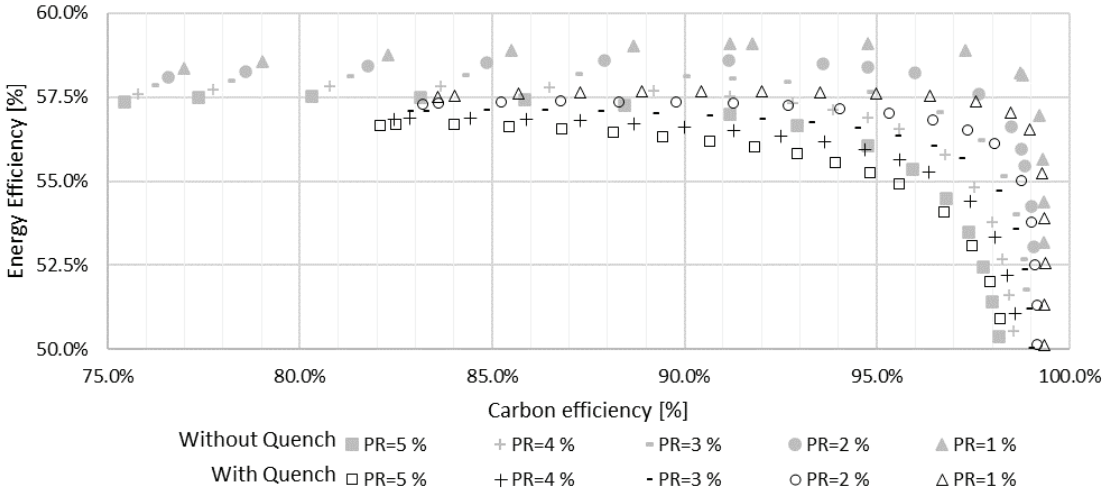

Figure 5. Energy efficiency over carbon efficiency the two different plants at different purge ratios (PR). Note: the grey, filled symbols denote the plant with hydrogen addition at low temperature

https://doi.org/10.52202/069564-0102

(without quench), while the black, empty symbols denote the addition at high temperature (with quench).

Figure 6 shows the electricity consumption in the two different plant layouts for purge ratios of 5 % and 1 %, respectively, for achieving a carbon efficiency of 95 %. It can first be seen that at higher purge ratios (Figure 6, left), more hydrogen was needed for producing the same amount of DME than for lower purge ratios (Figure 6,right), shown by the higher electricity consumption of the electrolyser. The higher amount of hydrogen in the system led also to a higher electricity consumption of the turbomachinery for the plant with hydrogen quench (6.1 vs. 5.7 MW), because more hydrogen needed to be compressed from ambient pressure to the high pressure of 85 bar for methanol synthesis.

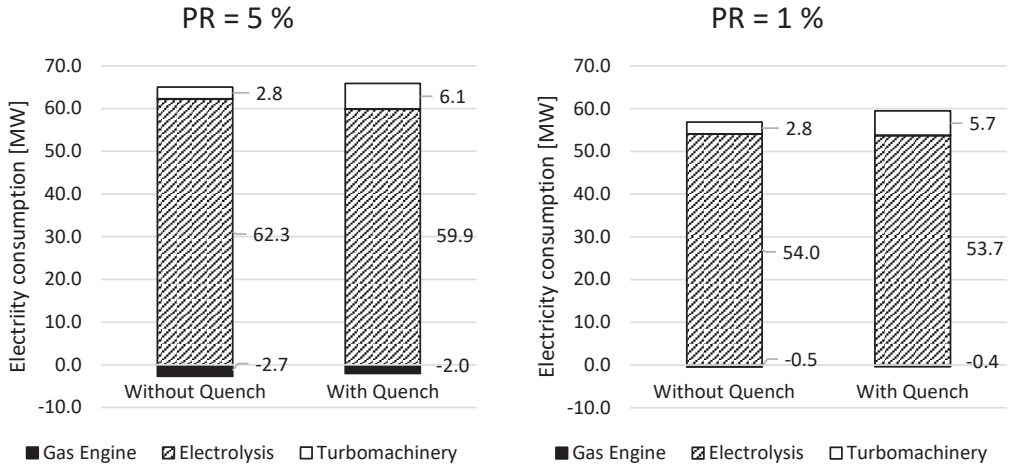

Figure 6. Electricity consumption and production of the different components in plants with a carbon efficiency of $\gamma_{tot} = 95$ %.

This effect was not seen for the plant without hydrogen quench, where the electricity consumption of the turbomachinery remained constant, due to two factors. Firstly, the electrolyser was operated at 30 bar, reducing the influence of the hydrogen on the overall electricity consumption in the turbomachinery. Secondly, the operation at 30 bar introduced the use of turbines for expanding the oxygen produced in the electrolyser, which reduced the electricity consumption with increasing hydrogen production. Additionally, for a purge rate of 5 % the electricity production in the gas engine was higher than at lower purge rate. The higher production derived from significantly more hydrogen and unconverted CO being purged and combusted in the gas engine, leading to both lower energy efficiency and carbon efficiency.

In general, higher energy efficiencies were achieved in the plants with hydrogen addition at low temperatures (without quench), as seen in Figure 5. At first, this may seem surprising, since there was more or equal as much hydrogen required to yield the same amount of DME, as seen in Figure 4. However, in Figure 6 it can be seen that for all purge rates, the higher electricity consumption for electrolysis in the plants without hydrogen quench was compensated by a lower electricity consumption in the turbomachinery, leading to a lower net electricity consumption for the same DME production. The increased electricity consumption for the plants with hydrogen quench derived from the necessity of operating the electrolysers at ambient pressure, leading to compression of hydrogen from ambient pressure to 85.1 bar (instead of 30 bar to 85.1 bar for the plants without hydrogen quench) and not having any electricity generation from expanding the produced oxygen in turbines. The electricity consumption in the 5-stage compression train was increased from 3.81 MW for the plant without hydrogen quench to 6.03 MW for the plant with hydrogen quench at $PR = 5\,\%$ and from 3.70 MW to 5.71 MW for $PR = 1\%$. The electricity production in the oxygen turbines for the plant without hydrogen quench was 1.09 MW for $PR = 5\,\%$ and 0.94 MW for $PR = 1\,\%$. The electricity consumption of the remaining turbomachinery, i.e. pumps and recycling compressor, was significantly smaller than the aforementioned consumption and production and their influence on the variation of the net electricity was negligible.

Lastly, we looked at the influence on the mole flow rate into the methanol reactor for three different carbon efficiencies, i.e. 82 %, 90 % and 95 % (Figure 7). The increases are shown as relative increases compared to a reference case as defined in eqs.(9) and (10). The reference case was the plant with hydrogen addition at high temperatures (with quench) from [8]. It had a purge ratio of 5 % and a carbon efficiency of 82 %.

https://doi.org/10.52202/069564-0102

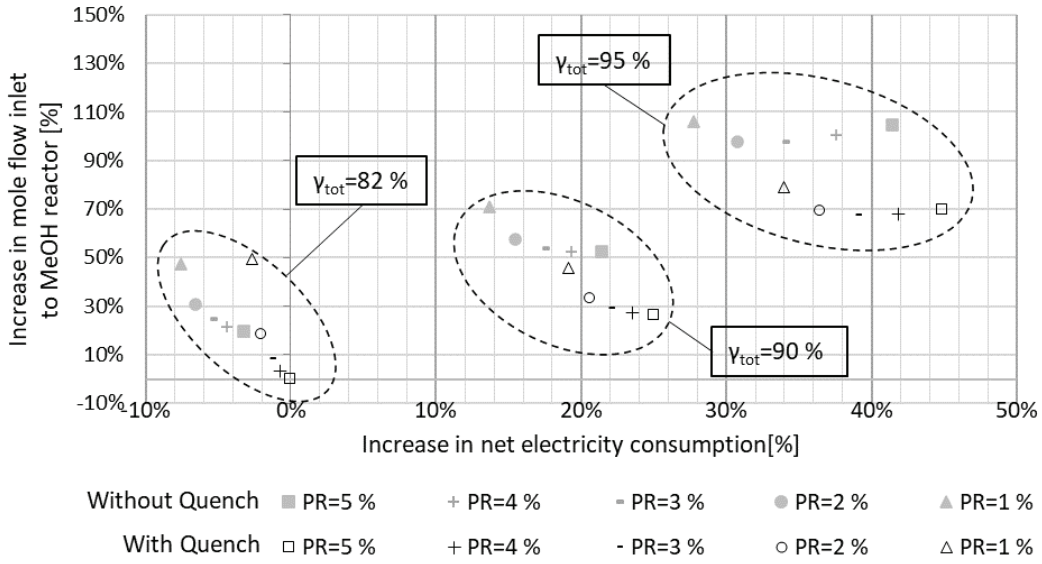

Figure 7. Increase in mole flow rate into the methanol reactor as an indicator for the reactor size over increase in net electricity consumption as an indicator for the operational cost for the different plants at varied purge ratios (PR) for three different carbon efficiencies γ_{tot}. Note: the grey, filled symbols denote the plant with hydrogen addition at low temperature (without quench), while the black, empty symbols denote the addition at high temperature (with quench).

In general, it can be seen that a reduction in purge ratio led to a lower electricity consumption, while the inlet mole flow rate to the methanol reactor increased. The reduction in electricity consumption was already explained above. The increase in mole flow rate to the reactor at lower purge ratios derived mainly from increased recycling the inert nitrogen, but also from a higher CO and CO_2 mole flow rate through the higher recycling. For a carbon efficiency of 95 % a change in the general trend for the mole flow into the reactor was observed, where the inlet mole flow rate initially decreases when reducing the purge ratio from 5 % before starting to increase again for lower purge ratios. The behaviour derived from requiring significantly more hydrogen to achieve a carbon efficiency of 95 % at higher purge ratios, leading to higher mole flow rates into the methanol reactor, despite recycling less nitrogen, CO and CO2.

Looking at the results for the plants with a carbon efficiency of 82 %, for the plant with hydrogen quench, the mole flow rate into the methanol reactor was increased by 50 % by reducing the purge ratio from 5 % to 1 %, while the electricity consumption was reduced by 2.6 %. When not including a hydrogen quench, the electricity consumption was reduced by 3.2 % and the reactor inlet mole flow rate was increased by 20 % for $PR = 5$ %, while for $PR = 1$ %, a reduction in 7.6 % at a mole flow rate increase of 47 % was achieved. It was observed that all plants without hydrogen quench consumed less electricity than any of the plants with hydrogen quench, while the reactor size was larger at purge ratios between 2 % and 5 %.

For the plants with a carbon efficiency of 90 %, the electricity consumption was higher than for the reference case, as expected, due to the higher hydrogen demand for achieving higher carbon efficiencies. The trends for the two plants looked similar to those for the lower carbon efficiency, but the differences in reactor size were smaller, as seen by the flatter curves. For the plant with hydrogen quench, the electricity consumption was increased by 25 % and 19 % for the plants with $PR = 5$ % and $PR = 1$ %, respectively, while the molar flow rate into the methanol reactor was increased by 27 % and 46 % compared to the reference case, respectively. For the plant without hydrogen quench, the increases in electricity consumption were 21 % and 14 % and for the mole flow rate 52 % and 71 %, respectively.

The highest electricity consumption and reactor size were found for the plants with a carbon efficiency of 95 %, due to the amount of hydrogen needed. The increase in electricity consumption was 45 % and 34 % for the plant with hydrogen quench at $PR = 5$ % and $PR = 1$ %, respectively, and 41 % and 25 % for the plant without hydrogen quench. The mole flow rate to the methanol reactor was increased by 70 % and 79 % for the plants with hydrogen quench and by 105 % and 106 % without hydrogen quench.

4. Discussion

https://doi.org/10.52202/069564-0102

The results showed that higher energy efficiencies were achieved for plants without hydrogen quench compared to the plants with hydrogen quench (see Figure 5). This derived from avoiding the compression of hydrogen from ambient pressures up to a methanol synthesis pressure of 85 bar. Instead, the hydrogen could be added at 30 bar, enabling pressurized operation of the alkaline electrolyser, reducing the electricity consumption by pumping water to 30 bar instead. Reducing the purge ratio from 5 % increased the energy efficiency of the plants, by better utilizing the hydrogen in the system, leading to a lower hydrogen demand and hence lower electricity consumption. The highest energy efficiency of the investigated plants with $\eta_{\mathrm{main}} = 59.1\ \%$ was achieved with the plant without hydrogen quench and purge ratio of 1 %. This energy efficiency was reached when adding between 0.28 kg/s and 0.32 kg/s of hydrogen to the system, yielding carbon efficiencies of around $\gamma_{tot} = 90 \ldots 95\ \%$. The energy efficiency was almost constant and always larger than $\eta_{\mathrm{main}} \geq 58.3\ \%$ in the range of carbon efficiencies of $\gamma_{tot} = 77 \ldots 98\ \%$. For carbon efficiencies higher than 98 %, the energy efficiency dropped rapidly.

For the plant with hydrogen quench and a purge ratio of 1 %, the energy efficiency was as high as $\eta_{\mathrm{main}} = 57.7\ \%$ in the range of carbon efficiencies $\gamma_{tot} = 88 \ldots 94\ \%$. The energy efficiency was always higher than $\eta_{\mathrm{main}} \geq 57\ \%$ in the range of $\gamma_{tot} = 82 \ldots 98\ \%$. Pressurized operation of the LT-CFB gasifier and the downstream POX would reduce the difference in energy efficiency between the plants with and without hydrogen quench, because this would enable to use pressurized electrolysis also for the plant with hydrogen quench. If the gasifier is pressurised to 30 bar, it is expected that the plants with quench would achieve higher energy efficiency than the plants without quench. Pressurization of the LT-CFB gasifier could be economically feasible for large-scale plants, because it would reduce the size of the component. However, challenges with the biomass feeding may arise. Additionally, it could perhaps impact the tar formation mechanisms in the pyrolysis reactor and increase the risk of tar condensation and subsequent damage of components.

The evaluation of the size of the methanol reactor, described by the mole flow rate into the reactor, showed that for carbon efficiencies of 90 % and lower, a higher energy efficiency (i.e. lower electricity consumption) required a larger methanol reactor. This denotes that there is a trade-off between the investment cost (reactor size) and the operational cost (electricity consumption) of the plants. An economic analysis of the plans would be necessary in order to quantify, which of the factors has a larger influence on the overall plant economics. At higher carbon efficiencies (e.g. 95 %) a different trend was observed, where higher purge ratios led to both higher electricity consumption and larger methanol reactor. There it was clearly beneficial to choose a small purge ratio.

The same trade-off was observed in the comparison between plants with and without hydrogen quench. In order to achieve the same carbon efficiency, the plants with hydrogen quench required more electricity, while the methanol reactor was smaller. It should however be considered, that for the plants with hydrogen quench additional investment would be required for the hydrogen quench. This would consist of either increasing the size of the POX reactor and adding a hydrogen injection or adding an additional reactor for the hydrogen quench after the POX. An economic comparison between the system is necessary for making a clear conclusion.

Lastly, it should be noted that using the mole flow rate into the methanol reactor as a measure for the size of the reactor gives a first estimate of the required investment of the methanol reactor. However, comparing inlet mole flows to the reactor enables only to compare the cross-sectional area of the reactor, i.e. the diameter of or the number of tubes in the reactor, since it is proportional to the volume flow rate into the reactor. The shown results could not be used for making any suggestions on required changes in the length of the reactor, because the length depends strongly on the kinetics of the methanol synthesis reactions. Since the inlet composition to the reactor varied strongly between the different plants, due to the variations in purge ratio, amount of hydrogen addition and the use of hydrogen quench, the use of a kinetic model for estimating the length of the reactor could give further insides into the influence of these parameters on the economic performance of the different plants.

5. Conclusion

In this work we investigated the influence of the amount of electrolytic hydrogen and the purge ratio of the gas after the vapour-liquid separator in the methanol system in two different DME production plants. Both plants produced DME from wheat straw gasification using two-stage DME synthesis, where methanol was synthesized in a first step, and then dehydrated to DME and water in a second step. The plants used a partial oxidation (POX) step after the gasifier for reforming and cracking the tar and hydrocarbons in the produced gas. The difference between the plants was the location of hydrogen addition. In the plants without hydrogen quench, the hydrogen was added after the gas from the POX was cooled and compressed to 30 bar. The gas hydrogen mixture was then compressed to 85 bar. In the plant with hydrogen quench, the hydrogen was added at high temperatures directly after the POX, leading to a spontaneous reverse water gas shift reaction, converting CO_2 and H_2 to CO and H_2O.

The analysis showed that increasing the amount of hydrogen in the system led to a higher DME production and hence a higher carbon efficiency. Carbon efficiencies higher than 98 % were achieved for all plants and

https://doi.org/10.52202/069564-0102

purge ratios. By reducing the purge ratio, the carbon efficiency was increased at constant hydrogen addition, Because the hydrogen in the system was used more efficiently. At the same time, it also increased the energy efficiency of the plants. The plants with hydrogen quench produced more DME then the plants without hydrogen quench, when using the same amount of hydrogen and purge ratio. Despite the lower hydrogen demand, the electricity consumption was higher for the plants with hydrogen quench, due to increased compression work. The compression work was lower for the plants without hydrogen quench, due to adding the hydrogen at 30 bar, enabling to pump water to the electrolyser instead of compressing the hydrogen.

Additionally, the changes in the required size of the methanol synthesis reactor were estimated by comparing the mole flow rate at the inlet of the methanol reactor. The analysis showed that for most of the cases, measures leading to an increase in energy and/or carbon efficiency led also to an increase in reactor size, highlighting a trade-off between investment cost (larger reactor) and operational cost (lower electricity consumption/higher DME production). A detailed economic analysis is proposed to be conducted for further insights into the economic performance of the plants.

6. Acknowledgments

This research project was financially funded by the Danish Ministry of Foreign Affairs under the project “Clean Shipping on Green Fuel” (administered by Danida Fellowship Centre, project code: 18-M10-DTU).

7. Nomenclature

A	Ash content, wt.-%	N	Nitrogen content, wt.-%
C	Carbon content, wt.-%	O	Oxygen content, wt.-%
H	Hydrogen content, wt.-%	PR	Purge ratio, %
HHV	Higher heating value, Btu/lb	S	Sulphur content, wt.-%
LHV	Lower heating value, MJ/kg	T	Temperature, °C
$\dot{m}$	Mass flow rate, kg/s	$\dot{W}$	Electric power, kW
$\dot{n}$	Mole flow rate, mole/s		

Greek symbols

γ	Carbon efficiency, %	η	Energy efficiency, %
ε	Relative increase, %	λ	Excess air ratio, -

Subscripts and superscripts

EL	Electricity consumption	mech	Mechanical
is	Isentropic	Reactor	Methanol reactor
main	Main products	tot	Total system

Abbreviations

DH	District heating	POX	Partial oxidation
DME	Dimethyl ether	PR	Purge ratio
HHV	Higher heating value	rWGS	Reverse water gas shift
LHV	Lower heating value	SNG	Synthetic natural gas
LT-CFB	Low temperature circulating fluidized bed	VL	Vapor-liquid
		VLE	Vapor-liquid equilibrium
MeOH	Methanol	VLLE	Vapor-liquid-liquid equilibrium
PH	Process heat		

8. References

[1] H. Lund *et al.*, “The role of sustainable bioenergy in a fully decarbonised society,” *Renew Energy*, vol. 196, pp. 195–203, Aug. 2022, doi: 10.1016/j.renene.2022.06.026.

[2] G. Venturini, A. Pizarro-Alonso, and M. Münster, “How to maximise the value of residual biomass resources: The case of straw in Denmark,” *Appl Energy*, vol. 250, pp. 369–388, 2019, doi: 10.1016/j.apenergy.2019.04.166.

[3] J. Ahrenfeldt, T. P. Thomsen, U. Henriksen, and L. R. Clausen, “Biomass gasification cogeneration - A review of state of the art technology and near future perspectives,” *Appl Therm Eng*, vol. 50, pp. 1407–1417, 2013, doi: 10.1016/j.applthermaleng.2011.12.040.

[4] V. Hansen, D. Müller-Stöver, J. Ahrenfeldt, J. K. Holm, U. B. Henriksen, and H. Hauggaard-Nielsen, “Gasification biochar as a valuable by-product for carbon sequestration and soil amendment,” *Biomass Bioenergy*, vol. 72, no. 1, pp. 300–308, 2015, doi: 10.1016/j.biombioe.2014.10.013.

[5] R. Kofler and L. R. Clausen, “Wheat straw based polygeneration systems integrating the electricity, heating and transport sector,” *Smart Energy*, vol. 2, 2021, doi: 10.1016/j.segy.2021.100015.

[6] R. Kofler and L. R. Clausen, “Exergy-based comparison of three wheat straw based biorefineries,” in *Proceedings of the 35th International Conference on Efficiency, Cost, Optimization, Simulation and Environmental Impact of Energy Systems 2022*, ECOS, 2022.

[7] T. A. Semelsberger, R. L. Borup, and H. L. Greene, “Dimethyl ether (DME) as an alternative fuel,” *J Power Sources*, vol. 156, no. 2, pp. 497–511, 2006, doi: 10.1016/j.jpowsour.2005.05.082.

[8] R. Kofler and L. R. Clausen, “Increasing carbon efficiency for DME production from wheat straw and renewable electricity – Analysis of 14 system layouts,” *Energy Convers Manag*, vol. 281, p. 116815, Apr. 2023, doi: 10.1016/j.enconman.2023.116815.

[9] F. Bustamante *et al.*, “High-Temperature Kinetics of the Homogeneous Reverse Water-Gas Shift Reaction,” *AIChE Journal*, vol. 50, no. 5, pp. 1028–1041, May 2004, doi: 10.1002/aic.10099.

[10] Aspen Technology, “Aspen Plus,” 2020. https://www.aspentech.com/en/products/engineering/aspen-plus

[11] P. Kaushal, T. Proell, and H. Hofbauer, “Application of a detailed mathematical model to the gasifier unit of the dual fluidized bed gasification plant,” *Biomass Bioenergy*, vol. 35, no. 7, pp. 2491–2498, 2011, doi: 10.1016/j.biombioe.2011.01.025.

[12] G. Soave, “Equilibrium constants from a modified Redkh-Kwong equation of state,” Pergamon Press, 1972.

[13] J. Schwartzentruber and H. Renon, “Extension of UNIFAC to High Pressures and Temperatures by the Use of a Cubic Equation of State,” *Ind Eng Chem Res*, vol. 28, no. 7, pp. 1049–1055, Jul. 1989, doi: 10.1021/ie00091a026.

[14] R. H. Perry and D. W. Green, *Perry’s Chemical Engineers’ Handbook*, 7th ed. McGraw-Hill, 1997.

[15] A. Eschenbacher *et al.*, “Catalytic upgrading of tars generated in a 100 kW th low temperature circulating fluidized bed gasifier for production of liquid bio-fuels in a polygeneration scheme,” *Energy Convers Manag*, vol. 207, 2020, doi: 10.1016/j.enconman.2020.112538.

https://doi.org/10.52202/069564-0102